range 18–42 GHz. Center frequencies of open end cavities using 0.218 mm wide lines on 0.272 mm thick alumina can be predicted to within 0.45%. In addition, a four cavity technique for measuring open end discontinuity capacitance and $\epsilon_{reff}^{M}(f)$ has been described.

References

[1] R. H. Jansen and L. Wiemer, "Full wave theory based development of MM-wave circuit models for microstrip open end, gap, step, bend and tee," in *1989 IEEE MTT-S Int. Microwave Symp. Dig.*, pp. 779–782.

[2] X. Zhang and K. K. Mei, "Time-domain finite difference approach to the calculation of the frequency-dependent characteristics of microstrip discontinuities," *IEEE Trans. Microwave Theory Tech.*, vol. 36, pp. 1775–1787, Dec. 1988.

[3] L. P. Dunleavy and P. B. Katehi, "Shielding effects in microstrip discontinuities," *IEEE Trans. Microwave Theory Tech.*, vol. 36, pp. 1767–1773, Dec. 1988.

[4] P. B. Katehi and N. G. Alexopoulos, "Frequency-dependent characteristics of microstrip discontinuities in millimeter-wave integrated circuits," *IEEE Trans. Microwave Theory Tech.*, vol. MTT-33, pp. 1029–1035, Oct. 1985.

[5] R. W. Jackson and D. M. Pozar, "Full-wave analysis of microstrip open-end and gap discontinuities," *IEEE Trans. Microwave Theory Tech.*, vol. MTT-33, pp. 1036–1042, Oct. 1985.

[6] J. X. Zheng and D. C. Chang, "Numerical modeling of chamfered bends and other microstrip junctions of general shape in MMIC's," in *1990 IEEE MTT-S Int. Microwave Symp. Dig.*, pp. 709–712.

[7] J. McLean, H. Ling, and T. Itoh, "Full wave modeling of electrically wide microstrip open end discontinuities via a deterministic spectral domain method," in *1990 IEEE MTT-S Int. Microwave Symp. Dig.*, pp. 1155–1158.

[8] T. Uwano, "Characterization of microstrip open end in the structure of a parallel-coupled stripline resonator filter," *IEEE Trans. Microwave Theory Tech.*, vol. 39, pp. 595–600, Mar. 1991.

[9] M. Kirschning, R. H. Jansen, and N. H. L. Koster, "Accurate model for open end effect of microstrip lines," *Electron. Lett.*, vol. 17, pp. 123–125, Feb. 1981.

[10] R. H. Jansen and N. H. L. Koster, "Accurate results on the end effect of single and coupled microstrip lines for use in microwave circuit design," *AEU*, vol. 34, pp. 453–459, 1980.

[11] T. Uwano, "Accurate characterization of microstrip resonator open end with new current expression in spectral-domain approach," *IEEE Trans. Microwave Theory Tech.*, vol. 37, pp. 630–633, Mar. 1989.

[12] R. Garg and I. J. Bahl, "Characteristics of coupled microstriplines," *IEEE Trans. Microwave Theory Tech.*, vol. MTT-27, pp. 700–705, July 1979.

[13] M. Kirschning and R. H. Jansen, "Accurate wide-range design equations for the frequency-dependent characteristic of parallel coupled microstrip lines," *IEEE Trans. Microwave Theory Tech.*, vol. MTT-32, pp. 83–90, Jan. 1984.

[14] T. C. Edwards, *Foundations for Microstrip Circuit Design*. New York: Wiley, 1981.

[15] R. A. York and R. C. Comton, "Experimental evaluation of existing CAD models for microstrip dispersion," *IEEE Trans. Microwave Theory Tech.*, vol. 38, pp. 327–328, Mar. 1990.

[16] Touchstone®, a software simulator for linear microwave and RF circuits, is a product of EEsof®, Westlake, Village, CA 91362. The microstrip line, microstrip line including open end effect, and microstrip coupled lines elements were modeled using algorithms referenced in the EEsof® Touchstone® 2.1 Element Catalog, pp. LEL-87 to LEL-131 and HOW-3.

[17] R. H. Jansen and M. Kirschning, "Arguments and an accurate model for the power-current formulation of microstrip characteristic impedance," *AEU*, vol. 37, pp. 108–112, 1983.

[18] W. J. Getsinger, "Measurement and modeling of the apparent characteristic impedance of microstrip," *IEEE Trans. Microwave Theory Tech.*, vol. MTT-31, pp. 624–632, Aug. 1983.

[19] M. Kirschning and R. H. Jansen, "Accurate model for effective dielectric constant of microstrip with validity up to millimetre wave frequencies," *Electron. Lett.*, vol. 18, pp. 272–273, Mar. 1982.

[20] T. S. Laverghetta, *Microwave Materials and Fabrication Techniques*. Norwood, MA: Artech House, 1984.

[21] H. J. Finlay, R. H. Jansen, J. A. Jenkins, and I. G. Eddison, "Accurate characterization and modeling of transmission lines for GaAs MMIC's," *IEEE Trans. Microwave Theory Tech.*, vol. 36, pp. 961–967, June 1988.

[22] M. Kobayashi, "A dispersion formula satisfying recent requirements in microstrip CAD," *IEEE Trans. Microwave Theory Tech.*, vol. 36, pp. 1246–1250, Aug. 1988.

[23] H. A. Atwater, "Test of microstrip dispersion formulas," *IEEE Trans. Microwave Theory Tech.*, vol. 36, pp. 619–621, Mar. 1988.

[24] R. B. Adler, L. J. Chu and R. M. Fano, *Electromagnetic Energy Transmission and Radiation*. New York: Wiley, 1960.

Scattering at an Offset Circular Hole in a Rectangular Waveguide

C. Sabatier

Abstract—**A solution is given for the problem of scattering at an offset circular to rectangular junction and at a thick diaphragm, with an offset circular aperture, in a rectangular waveguide. The method used, is mode matching for computing one discontinuity. The difficulty arising from the fact that the eigenmodes of the two waveguides are known in different coordinate systems is overcome by simple transformation for the evaluation of overlap integral between the eigenmodes of each waveguide. Experimental results validate this method.**

Introduction

Waveguide diaphragms with circular apertures are frequently used as matching elements in microwave circuits (cavity filters, waveguide to cavity coupling, etc). While centered holes have been investigated by many authors [1]–[3], the case of offset holes has not been addressed to our knowledge.

The discontinuity, presented Fig. 1, is investigated with the method of field expansion into eigenmodes [4], where the three types of overlap integrals are Vhh (TE modes in the two waveguides), Vee (TM modes in the two waveguides), Veh (TE modes in the first waveguide, TM modes in the second). The fourth overlap integral between TM modes in the first waveguide and TE modes in the second is zero [5].

The field expansion is performed on all TE and TM modes in the two waveguides because there is no symmetry in this problem.

Analysis

Since the common section between the two waveguides is circular ($b \geqq 2R$), the three overlap integrals have been computed in the first coordinate system noted O_1 in polar units (r_1, θ_1). Thus, all of the electric fields of the two waveguides must be written in this system. In fact, we write all fields in Cartesian units (x_1, y_1) and we take the Jacobian when we compute the different overlap integrals. For this reason, all field expressions given below are written in function of r_1 and θ_1, even in the Cartesian coordinate system. This method was given in [3] for a centered hole.

Manuscript received April 18, 1991; revised October 10, 1991.

The author is with the Centre National d'Etudes des Telecommunications, Fort de la Tete de Chien, 06320 La Turbie, France.

IEEE Log Number 9105445.

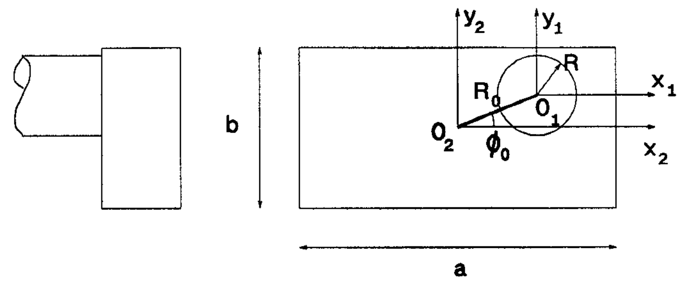

Fig. 1. An offset circular to rectangular junction.

The electric fields of the circular waveguide are easily expressed [3]:

TE_{kl} modes

$$\vec{e} = \sqrt{\frac{2}{\pi}}\,\frac{x'_{kl}}{2R}\,\frac{1}{\sqrt{1+\delta_{Ok}}}\,\frac{1}{\sqrt{(x'^2_{kl}-k^2)J_k^2(x'_{kl})}}\left|\begin{array}{l} J_{k-1}\left(\frac{x'_{kl}}{R}r_1\right)\sin(k-1)\theta_1 + J_{k+1}\left(\frac{x'_{kl}}{R}r_1\right)\sin(k+1)\theta_1 \\ J_{k-1}\left(\frac{x'_{kl}}{R}r_1\right)\cos(k-1)\theta_1 - J_{k+1}\left(\frac{x'_{kl}}{R}r_1\right)\cos(k+1)\theta_1 \end{array}\right|_{O_1(r_1,\,\theta_1)} \quad (1a)$$

TM_{kl} modes

$$\vec{e} = \sqrt{\frac{2}{\pi}}\,\frac{1}{2R}\,\frac{1}{J_{k+1}(x_{kl})}\,\frac{1}{\sqrt{1+\delta_{Ok}}}\left|\begin{array}{l} J_{k-1}\left(\frac{x_{kl}}{R}r_1\right)\sin(k-1)\theta_1 - J_{k+1}\left(\frac{x_{kl}}{R}r_1\right)\sin(k+1)\theta_1 \\ J_{k-1}\left(\frac{x_{kl}}{R}r_1\right)\cos(k-1)\theta_1 + J_{k+1}\left(\frac{x_{kl}}{R}r_1\right)\cos(k+1)\theta_1 \end{array}\right|_{O_1(r_1,\,\theta_1)} \quad (1b)$$

δ_{kl} is the Kronecker's delta ($\delta = 1$ if $k = l$, $\delta = 0$ otherwise)
x_{kl} is the lth root of $J_n(x)$,
x'_{kl} is the lth root of $J'_n(x)$.

The eigenmodes of the rectangular waveguides are separated into four cases according to the evenness of the modes on the x_2 and y_2 directions of the second coordinate system noted O_2. Only one case (i odd and j even for TE_{ij} or TM_{ij} modes) is given:

TE_{ij} modes

$$\vec{e} = \frac{2\pi(-1)^{(i+j+1)/2}}{\sqrt{ab}\,\sqrt{1+\delta_{Oj}}\,\sqrt{\left(\frac{i\pi}{a}\right)^2+\left(\frac{j\pi}{b}\right)^2}}\left|\begin{array}{l} \frac{j}{b}\sin\frac{i\pi}{a}x\sin\frac{j\pi}{b}y \\ \frac{i}{a}\cos\frac{i\pi}{a}x\cos\frac{j\pi}{b}y \end{array}\right|_{O_2(x_2,\,y_2)} \quad (2a)$$

TM_{ij} modes

$$\vec{e} = \frac{2\pi}{\sqrt{ab}\,\sqrt{\left(\frac{i\pi}{a}\right)^2+\left(\frac{j\pi}{b}\right)^2}}\left|\begin{array}{l} (-1)^{(i+j+1)/2}\frac{i}{a}\sin\frac{i\pi}{a}x\sin\frac{j\pi}{b}y \\ (-1)^{(i+j+1)/2}\frac{j}{b}\cos\frac{i\pi}{a}x\cos\frac{j\pi}{b}y \end{array}\right|_{O_2(x_2,\,y_2).} \quad (2b)$$

We transform these fields in function of (r_2, θ_2) in the same system by the method described in [3]:

TE_{ij} modes

$$\vec{e} = \frac{-2\pi(-1)^{(i+j+1)/2}}{r_{ij}\sqrt{ab}\,\sqrt{1+\delta_{Oj}}}\left|\begin{array}{l} \frac{2j}{b}\sum_{p=1}^{\infty}(-1)^p J_{2p}(r_2 r_{ij})\sin 2p\theta_2\sin 2p\theta_{ij} \\ \left(-\frac{i}{a}\right)\left[J_O(r_2 r_{ij}) + 2\sum_{p=1}^{\infty}(-1)^p J_{2p}(r_2 r_{ij})\cos 2p\theta_2\cos 2p\theta_{ij}\right] \end{array}\right|_{O_2(x_2,\,y_2)} \quad (3a)$$

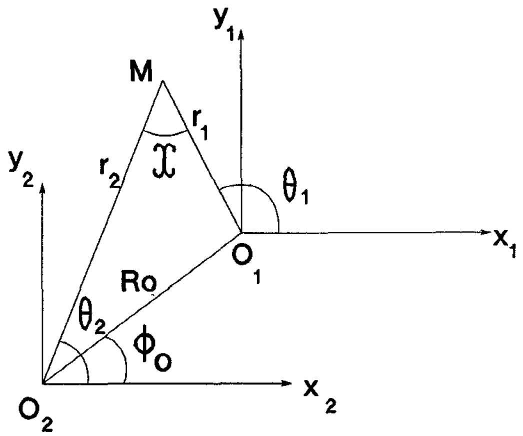

Fig. 2. Relations between the two coordinate systems.

TM_{ij} modes

$$\vec{e} = \frac{2\pi(-1)^{(i+j-1)/2}}{\sqrt{ab}\, r_{ij}} \left| \begin{array}{l} \dfrac{2i}{a} \sum_{p=1}^{\infty} (-1)^p J_{2p}(r_2 r_{ij}) \sin 2p\theta_2 \sin 2p\theta_{ij} \\ \dfrac{j}{b}\left[J_O(r_2 r_{ij}) + 2 \sum_{p=1}^{\infty} (-1)^p J_{2p}(r_2 r_{ij}) \cos 2p\theta_2 \cos 2p\theta_{ij}\right] \end{array} \right. \quad O_2(x_2, y_2)$$

$$r_{ij}^2 = \left(\frac{i\pi}{a}\right)^2 + \left(\frac{j\pi}{b}\right)^2, \quad \theta_{ij} = \tan^{-1}\left(\frac{aj}{ib}\right). \tag{3b}$$

The method for going from $O_2(r_2, \theta_2)$ to $O_1(r_1, \theta_1)$, which is the subject of this paper, is based on Graf's addition theorem [6].

The relation between the two radii and angles are (Fig. 2):

$$r_2 = \sqrt{R_O^2 + r_1^2 - 2R_O r_1 \cos(\pi - (\theta_1 - \phi_O))}$$

$$\theta_2 = \theta_1 - x. \tag{4}$$

We obtain, for the electric fields of the rectangular waveguide in the first coordinate system $O_1(x_1, y_1)$:

TE_{ij} modes

$$\vec{e} = \frac{2\pi(-1)^{(i+j-1)/2}}{r_{ij}\sqrt{ab}\sqrt{1+\delta_{Oj}}} \left| \begin{array}{l} \dfrac{2jE_1}{b} \\ -\dfrac{i}{a} E_2 \end{array} \right. \quad O_1(x_1, y_1) \tag{5a}$$

TM_{ij} modes

$$\vec{e} = \frac{2\pi(-1)^{(i+j-1)/2}}{r_{ij}\sqrt{ab}} \left| \begin{array}{l} \dfrac{2i}{a} E_1 \\ \dfrac{j}{b} E_2 \end{array} \right. \quad O_1(x_1, y_1)$$

$$E_1 = \sum_{p=1}^{\infty} (-1)^p \sin 2p\theta_{ij} \sum_{s=-\infty}^{\infty} J_s(r_{ij}R_O) J_{s+2p}(r_{ij}r_1) \cdot [\cos s(\pi + \phi_O) \sin (s+2p)\theta_1 - \sin s(\pi+\phi_O) \cdot \cos (s+2p)\theta_1]$$

$$E_2 = \sum_{s=-\infty}^{\infty} J_s(r_{ij}R_O) J_s(r_{ij}r_1) [\cos s(\pi+\phi_O) \cdot \cos s\theta_1 + \sin s(\pi+\phi_O) \cdot \sin s\theta_1] + 2 \sum_{p=1}^{\infty} (-1)^p \cos 2p\theta_{ij} \sum_{s=-\infty}^{\infty} J_s(r_{ij}R_O) J_{s+2p}(r_{ij}r_1) \cdot [\cos s(\pi+\phi_O) \cos (s+2p)\theta_1 + \sin s(\pi+\phi_O) \cdot \sin (s+2p)\theta_1]. \tag{5b}$$

Since all electric fields are expressed in the same coordinate system, we can easily compute the overlap integrals which are

$$V_{hh} = \iint_S \vec{e}_{kl}\vec{e}_{ij}\, dS \quad \left| \begin{array}{l} \vec{e}_{kl}\text{: (1a)} \\ \vec{e}_{ij}\text{: (5a)} \end{array} \right. \tag{6a}$$

$$V_{ee} = \iint_S \vec{e}_{kl}\vec{e}_{ij}\, dS \quad \left| \begin{array}{l} \vec{e}_{kl}\text{: (1b)} \\ \vec{e}_{ij}\text{: (5b)} \end{array} \right. \tag{6b}$$

$$V_{eh} = \iint_S \vec{e}_{kl}\vec{e}_{ij}\, dS \quad \left| \begin{array}{l} \vec{e}_{kl}\text{: (1a)} \\ \vec{e}_{ij}\text{: (5b).} \end{array} \right. \tag{6c}$$

S is the common section between the two waveguides (circular section in our case).

We obtain, for the three overlap integrals:

$$V_{hh} = \sqrt{\frac{2\pi}{ab}} \frac{2\pi x'_{kl}}{\left(\frac{x'_{kl}}{R}\right)^2 - r_{ij}^2} \frac{1}{\sqrt{1+\delta_{Ok}}\sqrt{1+\delta_{Oj}}} \frac{(-1)^{(i+j-1)/2}}{r_{ij}\sqrt{x'^2_{kl} - k^2}} \cdot \left[\left[\frac{x'_{kl}}{R} J_{k-1}(r_{ij}R) - \frac{r_{ij}}{R} J_k(r_{ij}R)\right] E_3 + \left[\frac{r_{ij}k}{x'_{kl}} J_k(x_{ij}R) - \frac{x'_{kl}}{R} J_{k+1}(r_{ij}R)\right] E_4\right] \tag{7a}$$

$$V_{ee} = \sqrt{\frac{2\pi}{ab}} \frac{2\pi}{\left(\frac{x_{kl}}{R}\right)^2 - r_{ij}^2} \frac{(-1)^{(i+j-1)/2}}{\sqrt{1+\delta_{Ok}}} J_k(r_{ij}R) E_5 \tag{7b}$$

$$V_{eh} = \sqrt{\frac{2\pi}{ab}} \frac{2x'_{kl}\pi}{\left(\frac{x'_{kl}}{R}\right)^2 - r_{ij}^2} \frac{(-1)^{(i+j-1)/2}}{\sqrt{x'^2_{kl} - k^2}} \frac{1}{\sqrt{1+\delta_{Ok}}} \frac{1}{r_{ij}} \cdot \left[\left[\frac{x'_{kl}}{R} J_{k-1}(r_{ij}R) - \frac{r_{ij}k}{x'_{kl}} J_k(r_{ij}R)\right] E_6 - \left[\frac{r_{ij}k}{x'_{kl}} J_k(r_{ij}R) - \frac{x'_{kl}}{R} J_{k+1}(r_{ij}R)\right] E_7\right] \tag{7c}$$

if $(r_{ij} \neq x/R)$ and

$$V_{hh} = \sqrt{\frac{2\pi}{ab}} \frac{R^2}{x'^2_{kl}} \frac{1}{\sqrt{1+\delta_{Oj}}} \frac{1}{\sqrt{1+\delta_{Ok}}} \frac{\pi(-1)^{(i+j-1)/2} J_k(x'_{kl})}{\sqrt{x'^2_{kl} - k^2}} \cdot [(x'^2_{kl} - k^2 + 2k)E_3 + (x'^2_{kl} - k^2 - 2k)E_4] \tag{8a}$$

$$V_{ee} = \sqrt{\frac{2\pi}{ab}} \frac{\pi R^2}{x_{kl}} J_{k+1}(x_{kl}) \frac{(-1)^{(i+j-1)/2}}{\sqrt{1+\delta_{Ok}}} E_5 \tag{8b}$$

$$V_{eh} = \sqrt{\frac{2\pi}{ab}} \frac{R^2}{x_{kl}} \frac{\pi(-1)^{(i+j-1)/2}}{\sqrt{x^2_{kl} - k^2}} \frac{J_k(x_{kl})}{\sqrt{1+\delta_{Ok}}} [(x^2_{kl} - k^2 + 2k)E_6 - (x^2_{kl} - k^2 - 2k)E_7] \tag{8c}$$

if $(r_{ij} = x/R)$, x is x'_{kl} or x_{kl} which depend on TE or TM modes in the circular waveguide.

$$E_3 = -\frac{i}{a} J_{k-1}(r_{ij}R_O) \cos(k-1)(\pi+\phi_O) + \sum_{p=1}^{\infty} (-1)^p J_{k-1-2p}(r_{ij}R_O) \cos(k-1-2p) \cdot (\pi+\phi_O)\left(\frac{j}{b}\sin 2p\theta_{ij} - \frac{i}{a}\cos 2p\theta_{ij}\right) - \sum_{p=1}^{\infty} (-1)^p J_{k-1+2p}(r_{ij}R_O) \cos(k-1+2p) \cdot (\pi+\phi_O)\left(\frac{j}{b}\sin 2p\theta_{ij} + \frac{i}{a}\cos 2p\theta_{ij}\right)$$

$$E_4 = \frac{i}{a} J_{k+1}(r_{ij}R_O) \cos(k+1)(\pi+\phi_O) + \sum_{p=1}^{\infty} (-1)^p J_{k+1-2p}(r_{ij}R_O) \cos(k+1-2p) \cdot (\pi+\phi_O)\left(\frac{j}{b}\sin 2p\theta_{ij} + \frac{i}{a}\cos 2p\theta_{ij}\right) - \sum_{p=1}^{\infty} (-1)^p J_{k+1+2p}(r_{ij}R_O) \cdot \cos(k+1+2p) \cdot (\pi+\phi_O)\left(\frac{j}{b}\sin 2p\theta_{ij} - \frac{i}{a}\cos 2p\theta_{ij}\right)$$

$$E_5 = \frac{j}{b}[J_{k-1}(r_{ij}R_O) \cdot \cos(k-1)(\pi+\phi_O) + J_{k+1}(r_{ij}R_O)\cos(k+1)(\pi+\phi_O)] + \sum_{p=1}^{\infty} (-1)^p J_{k-1-2p}(r_{ij}R_O) \cdot \cos(k-1-2p) \cdot (\pi+\phi_O)\left(\frac{j}{b}\cos 2p\theta_{ij} + \frac{i}{a}\sin 2p\theta_{ij}\right) + \sum_{p=1}^{\infty} (-1)^p J_{k-1+2p}(r_{ij}R_O) \cdot \cos(k-1+2p) \cdot (\pi+\phi_O)\left(\frac{j}{b}\cos 2p\theta_{ij} - \frac{i}{a}\sin 2p\theta_{ij}\right) + \sum_{p=1}^{\infty} (-1)^p J_{k+1-2p}(r_{ij}R_O) \cdot \cos(k+1-2p) \cdot (\pi+\phi_O)\left(\frac{j}{b}\cos 2p\theta_{ij} - \frac{i}{a}\sin 2p\theta_{ij}\right) + \sum_{p=1}^{\infty} (-1)^p J_{k+1+2p}(r_{ij}R_O) \cdot \cos(k+1+2p) \cdot (\pi+\phi_O)\left(\frac{j}{b}\cos 2p\theta_{ij} + \frac{i}{a}\sin 2p\theta_{ij}\right)$$

$$E_6 = \frac{j}{b} J_{k-1}(r_{ij}R_O) \cdot \cos(k-1)(\pi+\phi_O) + \sum_{p=1}^{\infty} (-1)^p J_{k-1-2p}(r_{ij}R_O) \cdot \cos(k-1-2p) \cdot (\pi+\phi_O)\left(\frac{i}{a}\sin 2p\theta_{ij} + \frac{j}{b}\cos 2p\theta_{ij}\right) + \sum_{p=1}^{\infty} (-1)^p J_{k+2p-1}(r_{ij}R_O) \cdot \cos(k+2p-1) \cdot (\pi+\phi_O)\left(\frac{j}{b}\cos 2p\theta_{ij} - \frac{i}{a}\sin 2p\theta_{ij}\right)$$

$$E_7 = \frac{j}{b} J_{k+1}(r_{ij}R_O) \cdot \cos(k+1)(\pi+\phi_O) + \sum_{p=1}^{\infty} (-1)^p J_{k+1-2p}(r_{ij}R_O) \cdot \cos(k+1-2p) \cdot (\pi+\phi_O)\left(\frac{j}{b}\cos 2p\theta_{ij} - \frac{i}{a}\sin 2p\theta_{ij}\right) + \sum_{p=1}^{\infty} (-1)^p J_{k+2p+1}(r_{ij}R_O) \cdot \cos(k+2p+1) \cdot (\pi+\phi_O)\left(\frac{i}{a}\sin 2p\theta_{ij} + \frac{j}{b}\cos 2p\theta_{ij}\right).$$

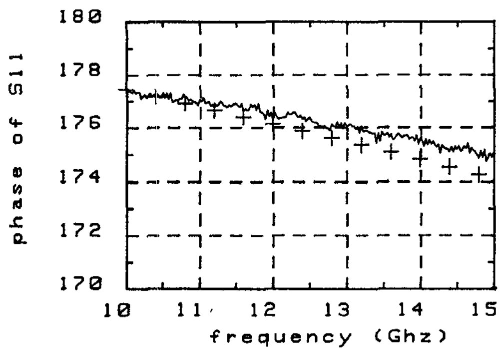

Fig. 3. Comparison for the phase of the reflection coefficient of a small hole in a WR75 waveguide.

The others cases, which depend on the evenness of i and j of TE and TM modes of the rectangular waveguide, are evaluated in the same way. The same formulas are analytically obtained if $R_O = \phi_O = 0$ as in the centered junction. The infinite sums decreases very rapidly, only 4 or 5 terms are computed for an error $< 10^{-6}$.

For cascaded transitions, the evanescent fields are taken into account between each junction [4].

Results

The first comparison is made for a small hole of 5 mm in diameter, put in a WR75 waveguide. Its thickness is 2 mm. The offsets are $R_O = 2.5$ mm and $\phi_O = 0$ degree. If the magnitude of the reflection coefficient is 1 in all the bandwidth of the rectangular waveguide, the phase of this parameter decreases when the frequency (10–15 GHz) increases. The comparison between experimental values (solid line) and theoretical values (symbols) of the phase presented in Fig. 3, is excellent.

Another test is made for a hole whose diameter is equal to the height of the WR75 waveguide. It has the same thickness as in the first case. The offsets between the two coordinate systems are $R_O = 4$ mm and $\phi_O = 0$ degree. The measured (solid line) and computed (symbols) reflection coefficients are compared in Fig. 4 in magnitude and in phase. Good agreement is obtained.

Convergence

The main setback of the modal matching approach is the relative convergence problem. Regarding this problem, the variation of the reflection coefficient is investigated in function of the number of TE and TM modes taken into account. The case used for this study is the second experimental test. Amplitude and phase are presented Table I (frequency 11 GHz, experimental data: 0.989746; 163.104 degrees) and Table II (frequency 14 GHz, experimental data: 0.940338; 149.727 degrees). The number of TE and TM modes selected, affects the theoretical values as predicted. 22 TE modes and 14 TM modes were taken into account for the first comparison with experimental values (the error is less, than 1 degree); only 14 TE modes and 6 TM modes are sufficient to obtain convergence in the second case. The number of modes necessary to achieve correct theoretical values increases as the radius of the circular waveguide decreases.

Conclusion

In this letter, a simple method is developed for taking into account offset circular hole in rectangular waveguide based on Graf's addition theorem. Analytically, the formulas given for the centered

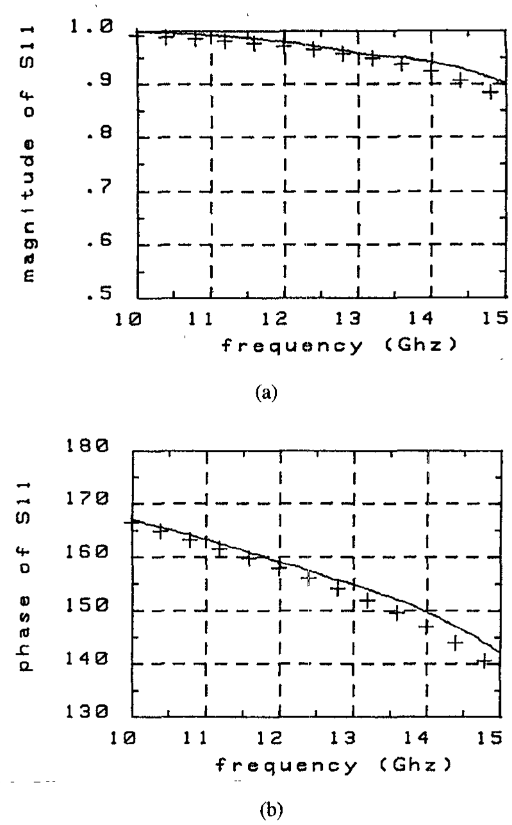

Fig. 4. Magnitude and phase of the reflection coefficient for a diaphragm with an offset circular hole in a rectangular waveguide.

TABLE I

TE \ TM	6	14	22	30
6	0.964223 157.765	0.963931 157.699	0.963712 157.647	0.963704 157.645
14	0.981161 162.16	0.98106 162.127	0.980919 162.08	0.980912 162.078
22	0.981545 162.277	0.981451 162.247	0.981311 162.199	0.981305 162.197
30	0.982863 162.744	0.982278 162.716	0.982659 162.673	0.982654 162.672

TABLE II

TE \ TM	6	14	22	30
6	0.842836 136.715	0.840448 136.453	0.838674 136.254	0.838593 136.246
14	0.922106 146.764	0.921314 146.639	0.920217 146.464	0.920159 146.455
22	0.923472 146.969	0.922724 146.85	0.921623 146.673	0.921567 146.665
30	0.929271 147.953	0.928607 147.844	0.927665 147.686	0.927621 147.678

transition are retrieved when the offsets are zero. However, a large number of modes is required to obtain precise values.

References

[1] H. A. Bethe, "Theory of diffraction by small holes," *Phys. Rev.*, vol. 66, pp. 163–182, Oct. 1944.
[2] N. Marcuwitz, *Waveguide Handbook*. New York: McGraw-Hill, 1951.
[3] J. D. Wade and R. H. Macphie, "Scattering at circular to rectangular waveguide junctions," *IEEE Trans. Microwave Theory Tech.*, vol. MTT-34, pp. 1085–1091, 1986.
[4] H. Patzelt and F. Arndt, "Double plane steps in rectangular waveguides and their application for transformers, irises and filters," *IEEE Trans. Microwave Theory Tech.*, vol. MTT-30, pp. 771–776, 1982.
[5] R. E. Collin, *Field Theory of Guided Waves*. New York, McGraw-Hill, 1960.
[6] M. Abramowitz and I. A. Stegun, *Handbook of Mathematical Functions*. New York: Dover, 1965.

Moment Method Formulation of Thick Diaphragms in a Rectangular Waveguide

Amlan Datta, B. N. Das, and Ajoy Chakraborty

Abstract—**The paper presents a method of determination of the electrical characteristics of two thick apertures in a rectangular waveguide. The coupled integral equations resulting from the boundary condition of the magnetic field at the four interfaces are transformed into matrix equations using method of moments. The numerical data on reflection and transmission coefficients are evaluated. Comparison between theoretical and experimental results is presented.**

I. Introduction

The analysis of waveguide discontinuities in the form of thin and thick apertures has been carried out by a number of workers [1]–[4]. Marcuvitz used variational formulation for determining the equivalent network parameters of diaphragms with zero axial thickness and supplied experimental data on complex reflection coefficient for a diaphragm of thickness 0.08 cm in a rectangular waveguide [1]. The variational formulation was also applied to cylindrical posts with small circular and rectangular cross-section. The reference plane for lumped equivalent network representation of this structure was taken as the plane of symmetry of the obstacle. The application of this form is limited to obstacles having maximum linear dimension less than 10% of the waveguide broad dimension and for location with minimum distance of 30% of the guide broad dimension from the side wall. The analysis of apertures with finite axial thickness has also been carried out by Marcuvitz using the static method [1, Sect. 8.7–8.8]. The results are accurate for axial thickness much greater than the aperture width. In this case, however, the reference plane for lumped equivalent network representation has not been properly indicated presumably because of application of the static method. Collin has suggested a method for determination of the parameters of the equivalent T network of an inductive diaphragm with finite axial thickness [2]. The analysis is based on evaluation of the eigenvalues of the impedance matrix of the T network. In addition to some confusion about the reference plane for the network representation, the authors didn't find the method convenient for computation. The moment method formulation has recently been applied by Scharstein et al. [3] and Auda and Harrington [4] for thin diaphragms in circular and rectangular waveguides. The analysis of Scharstein et al. for an iris in a circular waveguide is based on aperture field formulation and of Auda et al. for thin iris in a rectangular waveguide is based on obstacle current method. In view of the potential application of the above structure for microwave systems, it has been felt desirable to present a method of analysis which is free from these limitations.

Manuscript received May 20, 1991; revised October 10, 1991.
The authors are with the Department of Electronics and Electrical Communication Engineering, Indian Institute of Technology, Kharagpur, Pin-721302, India.
IEEE Log Number 9105444.

In the present work attention has been paid to evaluate the electrical characteristics of thick double apertures in a rectangular waveguide. The analysis is carried out using moment method and aperture field formulation. The aperture field method is used in lieu of obstacle current method because of the following advantages. The application of aperture field method permits use of entire domain sinusoidal basis function which gives a faster convergence than the subsectional basis function used in obstacle current method. The application of Galerkin's technique leads to a symmetric moment matrix which reduces the computation time appreciably. Same formulation can be applied to both inductive as well as capacitive obstacles.

The rectangular aperture with finite axial thickness has been represented as a short rectangular waveguide. The axial thickness is accounted for by introducing higher order waveguide modes in the short waveguide connecting the input and output region [5]. The expressions for the magnetic field generated due to the aperture fields in the two interfaces are derived using modal expansion method [6, Sect. 4.9]. The coupled integral equations resulting from the boundary condition of the magnetic field at the four interfaces are transformed into matrix equation using Galerkin's method. The comparisons between the theoretical results is presented. Theoretical and experimental data are also determined for a single aperture for the sake of comparison with those presented by Marcuvitz.

II. Analysis

Fig. 1(a) shows the cross-sectional view of a rectangular waveguide containing two apertures. The longitudinal-sectional view of the same is shown in Fig. 1(b).

For the purpose of analysis the apertures are considered as sections of waveguides as shown in Fig. 1(b). The modes existing in the two apertures are assumed to be of the type $TE_{0i}(i = p, q)$ [5].

Using modal expansion formulation suggested by Harrington [6, Sect. 4.9], the expressions for the back scattered ($z \leq -t/2$) and forward scattered ($z \geq t/2$) magnetic field at $z = -t/2$ and $z = t/2$ are expressed as

$$H_i(e_p) = V_n\,[\text{sinc}\,\{R_{np}(w_1)\}\cos\{S_{np}(c_1)\} - \text{sinc}\,\{T_{np}(w_1)\}\cos\{U_{np}(c_1)\}]\sin\left(\frac{\pi y}{b}\right) \tag{1}$$

$$H_i(e_q) = V_n\,[\text{sinc}\,\{R_{nq}(w_2)\}\cos\{S_{nq}(c_2)\} - \text{sinc}\,\{T_{nq}(w_2)\}\cos\{U_{nq}(c_2)\}]\sin\left(\frac{\pi y}{b}\right) \tag{2}$$

$$H_o(e_p) = -H_i(e_p) \quad \text{and} \quad H_o(e_q) = -H_i(e_q) \tag{3}$$